Measurement of $R = \sigma_L/\sigma_T$ and the separated longitudinal and transverse structure functions in the nucleon-resonance region

Y. Liang,[1,7] V. Tvaskis,[7,19] M. E. Christy,[7] A. Ahmidouch,[14] C. S. Armstrong,[19] J. Arrington,[2,24] R. Asaturyan,[23] S. Avery,[7] O. K. Baker,[7,19] D. H. Beck,[8] H. P. Blok,[21] C. W. Bochna,[8] W. Boeglin,[4,19] P. Bosted,[1,19] M. Bouwhuis,[8] H. Breuer,[9] D. S. Brown,[9] A. Bruell,[10] R. D. Carlini,[19] J. Cha,[12] N. S. Chant,[9] A. Cochran,[7] L. Cole,[7] S. Danagoulian,[14] D. B. Day,[20] J. Dunne,[12] D. Dutta,[10,12] R. Ent,[19] H. C. Fenker,[19] B. Fox,[3] L. Gan,[7] H. Gao,[10] K. Garrow,[19] D. Gaskell,[2,16] A. Gasparian,[7] D. F. Geesaman,[2] R. Gilman,[18,19] P. L. J. Guèye,[7] M. Harvey,[7] R. J. Holt,[8] X. Jiang,[18] M. Jones,[19] C. E. Keppel,[7,19] E. Kinney,[3] W. Lorenzon,[11] A. Lung,[19] D. J. Mack,[19] P. Markowitz,[4,19] J. W. Martin,[10] K. McIlhany,[10] D. McKee,[13] D. Meekins,[5,19] M. A. Miller,[8] R. G. Milner,[10] J. H. Mitchell,[19] H. Mkrtchyan,[23] B. A. Mueller,[2] A. Nathan,[8] G. Niculescu,[15] I. Niculescu,[6] T. G. O'Neill,[2] V. Papavassiliou,[13,19] S. F. Pate,[13,19] R. B. Piercey,[12] D. Potterveld,[2] R. D. Ransome,[18] J. Reinhold,[4,19] E. Rollinde,[19,22] O. Rondon,[20] P. Roos,[9] A. J. Sarty,[5] R. Sawafta,[14] E. C. Schulte,[8] E. Segbefia,[7] C. Smith,[20] S. Stepanyan,[23] S. Strauch,[18] V. Tadevosyan,[23] L. Tang,[7,19] R. Tieulent,[9,19] A. Uzzle,[7] W. F. Vulcan,[19] S. A. Wood,[19] F. Xiong,[10] L. Yuan,[7] M. Zeier,[20] B. Zihlmann,[20] and V. Ziskin[10,17]

[1]*American University, Washington, D.C. 20016, USA*
[2]*Argonne National Laboratory, Argonne, Illinois 60439, USA*
[3]*University of Colorado, Boulder, Colorado 80309, USA*
[4]*Florida International University, University Park, Florida 33199, USA*
[5]*Florida State University, Tallahassee, Florida 32306, USA*
[6]*The George Washington University, Washington, D.C. 20052, USA*
[7]*Hampton University, Hampton, Virginia 23668, USA*
[8]*University of Illinois, Champaign-Urbana, Illinois 61801, USA*
[9]*University of Maryland, College Park, Maryland 20742, USA*
[10]*Massachusetts Institute of Technology, Cambridge, Massachusetts 02139, USA*
[11]*University of Michigan, Ann Arbor, Michigan 48109, USA*
[12]*Mississippi State University, Mississippi State, Mississippi 39762, USA*
[13]*New Mexico State University, Las Cruces, New Mexico 88003, USA*
[14]*North Carolina A & T State University, Greensboro, North Carolina 27411, USA*
[15]*Ohio University, Athens, Ohio 45071, USA*
[16]*Oregon State University, Corvallis, Oregon 97331, USA*
[17]*Rensselaer Polytechnic Institute, Troy, New York 12180, USA*
[18]*Rutgers University, New Brunswick, New Jersey 08855, USA*
[19]*Thomas Jefferson National Accelerator Facility, Newport News, Virginia 23606, USA*
[20]*University of Virginia, Charlottesville, Virginia 22901, USA*
[21]*Vrije Universiteit, 1081 HV Amsterdam, The Netherlands*
[22]*College of William and Mary, Williamsburg, Virginia 23187, USA*
[23]*Yerevan Physics Institute, 375036, Yerevan, Armenia*
[24]*Lawrence Berkeley National Laboratory, Berkeley, California 94720, USA*

(Received 15 December 2021; accepted 9 June 2022; published 17 June 2022)

We report on a detailed study of longitudinal strength in the nucleon resonance region, presenting new results from inclusive electron-proton cross sections measured at Jefferson Lab Hall C in the four-momentum transfer range $0.2 < Q^2 < 5.5$ GeV^2. The data have been used to accurately perform 167 Rosenbluth-type longitudinal/transverse separations. The precision $R = \sigma_L/\sigma_T$ data are presented here, along with the first separate values of the inelastic structure functions F_1 and F_L in this regime. The resonance longitudinal component is found to be significant, both in magnitude and in the existence of defined mass peaks. Additionally, quark-hadron duality is here observed above $Q^2 = 1$ GeV^2 in the separated structure functions independently.

DOI: 10.1103/PhysRevC.105.065205

I. INTRODUCTION

The description of hadrons and their excitations in terms of elementary quark and gluon constituents continues to be one of the fundamental challenges in physics today. Considerable information on nucleon structure has been extracted over the past few decades from separations of inclusive

lepton-nucleon cross sections into longitudinal and transverse structure functions. The original experimental observation [1] of the vanishing ratio $R = \sigma_L/\sigma_T$, the ratio of the contributions to the measured cross section from longitudinally and transversely polarized virtual photon scattering, respectively, as measured in deep inelastic scattering (DIS), provided the first evidence of the fundamental spin-1/2 nature of the partons [2]. Since that time, separated structure functions have been measured in DIS over a wide range of four-momentum transfer, Q^2, and Bjorken scaling variable $x = Q^2/2M\nu$, where $\nu = E - E'$ is the electron energy transfer, and M is the proton mass [1,3–6]. For example, measurements of the purely longitudinal structure function F_L at low x from HERA have provided direct access to gluon distributions [7].

The quantity R is expressed in terms of the fundamental nucleon structure functions F_1 (purely transverse), F_L (purely longitudinal), and F_2 (combined longitudinal and transverse) as follows:

$$R \equiv \frac{\sigma_L}{\sigma_T} \equiv \frac{F_L}{2xF_1} = \frac{F_2}{2xF_1}\left(1 + \frac{4M^2x^2}{Q^2}\right) - 1. \qquad (1)$$

Within the framework of the naive parton model with spin-1/2 partons, $F_2 = 2xF_1$ (the Callan-Gross relationship [2]), and R is given by $4M^2x^2/Q^2$. By allowing the partons in this model to have an intrinsic transverse momentum p_T and a nonzero mass, the value of R is increased [8].

Precision measurements of R are necessary for several fundamental measurements. Extractions of the structure function F_2, or of the purely longitudinal or transverse structure functions, F_L and F_1, from cross-section measurements have historically depended on assumptions for R [4]. The uncertainties introduced by this assumption are highly ε-dependent, where ε is the relative longitudinal polarization of the virtual photon in the electron-nucleon scattering process [9]. This extraction is insensitive to R only for $\varepsilon = 1$, where the cross section is directly proportional to F_2. However, much of the world's high-precision resonance region data on F_2 come from measurements at much smaller values of ε, where the uncertainties introduced by R can be significant.

Uncertainties in the separation of unpolarized structure functions also have a direct impact on the extraction of the spin structure functions from spin-asymmetry measurements in electron scattering. Additionally, precision measurements of R can greatly aid efforts to develop decisive global descriptions of existing inclusive electroproduction data at moderate to high x and Q^2, necessary for lepton-nucleon scattering model development, structure function evolution studies, and accurate radiative correction calculations.

Very few measurements of R have been made in the nucleon resonance region [3,4,10,12]. Here, the quantity and precision of the existing data (prior to this work) were such that it was impossible to study either the mass-squared ($W^2 = M^2 + 2M\nu - Q^2$) or Q^2 dependencies of the separated longitudinal and transverse resonant structure. This is because such extractions require multiple precision measurements of the cross section at fixed Q^2 and W^2, allowing for the extraction of the longitudinal and transverse cross section from the $\varepsilon = 0$ limit and the slope in ε, respectively. If σ_L is very large (or very small) compared to σ_T, then one term will dominate the cross section, making it difficult to extract the smaller term. In addition, a large ε, needed to have good sensitivity to σ_L/σ_T, and a clean measurement of σ_L both rely on having precise data at low ε values. This corresponds to large scattering angles where measurements are often limited by small cross sections.

In a resonance excitation probed at moderate momentum transfer, large values of R and, correspondingly, F_L, are possible, due to gluon exchanges between the quarks. These effects, as well as the longitudinal character of individual resonances, are accessible via precision measurements of R. There have been measurements of R on the proton (and deuteron) in the DIS region [1,3–6], as well as studies of R in the DIS and resonance region [11–13] on nuclei. The results presented here represent the first detailed study of longitudinal strength in the full nucleon resonance region, to investigate nucleon resonance structure, and nucleon structure function behavior.

In perturbative quantum chromodynamics (pQCD), $F_L \propto \alpha_s$, and thus R is expected to decrease logarithmically with increasing Q^2 [14–16]. At low Q^2, Q^{-2}-type dynamic higher twist power corrections, interactions in which the struck quark exchanges a gluon with one of the spectator quarks in the scattering process, are expected to be a significant contribution to R. Additionally, kinematic higher twist effects originating from the binding of the quarks in the nucleon (target mass effects), are expected to be large. It has been previously reported [6] that R measured at intermediate Q^2 in the DIS regime [1,4–6] is higher than next-to-leading-order pQCD predictions, even with the inclusion of target mass corrections. This enhanced strength in R relative to pQCD was argued to be an observation of nonperturbative higher twist effects [5,6].

In contrast, more recent quantitative studies [17–22] of quark-hadron duality in the structure function F_2 suggest that, even in the resonance region, nonperturbative dynamic higher twist effects tend to be small for Q^2 as low as 1 GeV^2 when the structure function is averaged over any of the prominent resonance regions. That is, even though the function exhibits resonance (hadronic) structure, it tends to average to a global scaling curve consistent with expectations from DIS data and perturbative QCD (hence the term quark-hadron duality).

II. EXPERIMENT OVERVIEW

The experiment (E94-110 [23]) ran in Hall C at the Thomas Jefferson National Accelerator Facility (Jefferson Lab, or JLab). An electron beam with a near constant current of 60 μA was provided by the CEBAF accelerator with seven different energies ranging from 1.2 to 5.5 GeV. Incident electrons were scattered from a 4-cm-long liquid hydrogen target and detected in the high momentum spectrometer (HMS), over an angular range $12.9^\circ < \theta < 79.9^\circ$. The combination of high energy, high luminosity, and well-understood large-acceptance spectrometers allowed for precise longitudinal and transverse extractions to be performed over a the full resonance region for a significant range of Q^2 values. This also provides a large range in ε, maximizing the sensitivity of the separations over most of the kinematic range of the experiment.

To account for backgrounds from π^0 production and decay into two photons and subsequent electron-positron pairs, positrons were measured in the short orbit spectrometer (SOS) and also intermittently in the HMS. Other backgrounds included electron scattering from the aluminum walls of the cryogenic target cell, as well as electroproduced negatively charged pions. Events from the former were subtracted by performing substitute empty target runs, while events from the latter were identified and removed by the use of both a gas Cherenkov counter and an electromagnetic calorimeter. In all aspects of this experiment, particular attention was given to demonstrable systematic uncertainty minimization. For more details regarding the analysis and the Hall C apparatus employed in this experiment, see Refs. [24,25].

III. DATA ANALYSIS

The inclusive double differential cross section for each energy and angle bin within the spectrometer acceptance was determined from

$$\frac{d\sigma}{d\Omega dE'} = \frac{Y_{\rm corr}}{L\Delta\Omega\Delta E'}, \tag{2}$$

where $\Delta\Omega$ ($\Delta E'$) is the bin width in solid angle (scattered energy), L is the total integrated luminosity, and $Y_{\rm corr}$ is the final corrected yield of events. To obtain $Y_{\rm corr}$, the electron events were binned in small W and θ bins. This raw yield was corrected for the acceptance of the spectrometer in the bin (as determined from detailed Monte Carlo simulations), detector efficiencies, data acquisition live time, background contributions, and radiative corrections. A cross-section model was then used to correct for the difference between this cross section averaged over the θ bins and the value at the central spectrometer angle, and the cross section for a specific W bin was taken to be the weighted average of the values for the different θ bins.

Radiative corrections include the bremsstrahlung, vertex corrections, and loop diagrams standard to electron scattering experiments. These corrections were calculated following the prescription of Ref. [5], using structure function parametrizations from [4,26] and form factors from [27]. No corrections were made for higher order radiative processes involving two photon exchange, since no complete inelastic calculations for such effects. In addition, the impact on the extraction of σ_L is enhance by a factor of order $1/R$, which is much smaller in this case ($R \approx 3$) than for the high-Q^2 elastic form factor extractions ($R \ll 0.1$) where large two-photon exchange effects have been observed [28,29]. Moreover, our data set significant limits on the presence of nonlinear contributions, suggesting deviations from linearity below the 2% level over the entire kinematic range of our measurement [30], consistent with calculations that suggest that two-photon contributions in resonance production are relatively small and nearly linear in ε [29].

To minimize dependence on the model used to compute both the bin centering and the radiative correction, the following iterative procedure was employed: a starting model was used to compute the corrections; the data thus obtained were fit to obtain a new model and this resultant new model was then employed to recompute the original corrections and reextract the cross sections. These steps were repeated until the fitting yielded no further changes. Differing starting models were used to verify that the final cross sections were independent of the starting model within 0.6%. A positive byproduct of this approach is the availability of a new resonance region fit, including both resonances and nonresonant contributions, which describes the data presented here to better than 3% [31].

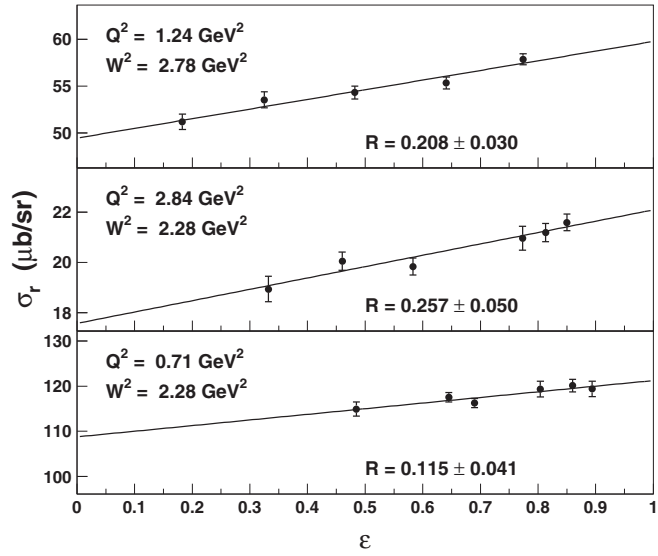

FIG. 1. Representative Rosenbluth plots for the kinematics indicated.

Typical cross-section statistical uncertainties per energy bin were less than 1% with systematic errors, uncorrelated in ε, of 1.6% [24]. The total systematic scale uncertainty in the cross-section measurements was 1.9%. The full cross-section sample consisted of 32 scans across the mass-squared range $M^2 < W^2 < 4$ GeV^2. Measurements at over 1,000 distinct W^2, Q^2 and ε points were obtained, allowing for longitudinal and transverse separations to be performed at 167 fixed W^2, Q^2 values with typically between 3 and 5 ε points in each separation.

The extractions of purely longitudinal and transverse cross sections and structure functions were accomplished via the Rosenbluth technique [32], where measurements are made over a range in ε at fixed x, Q^2, and the reduced cross section, $\sigma_r = d\sigma/\Gamma = \sigma_T + \varepsilon\sigma_L = \sigma_T(1 + \varepsilon R)$ is fit linearly with ε. Here, Γ is the transverse virtual photon flux in the electron-nucleon scattering process. Both ε and Γ were calculated from the measured kinematic variables. The intercept of such a fit gives the transverse cross section σ_T [and therefore the structure function $F_1(x, Q^2)$], while the slope gives the longitudinal cross section σ_L, from which can be extracted the structure functions $R(x, Q^2)$ and $F_L(x, Q^2)$. Because R is determined by the slope of the fit, relative to σ_T, the uncertainty in the extracted value of R (and likewise, F_L) is dominated by the uncorrelated uncertainties in the cross sections versus ε. Typical example Rosenbluth plots are shown Fig. 1.

Prior to a separation being performed, data within a Q^2 range of ± 0.5 GeV^2 and W^2 range of ± 0.05 GeV^2 for $W^2 <$

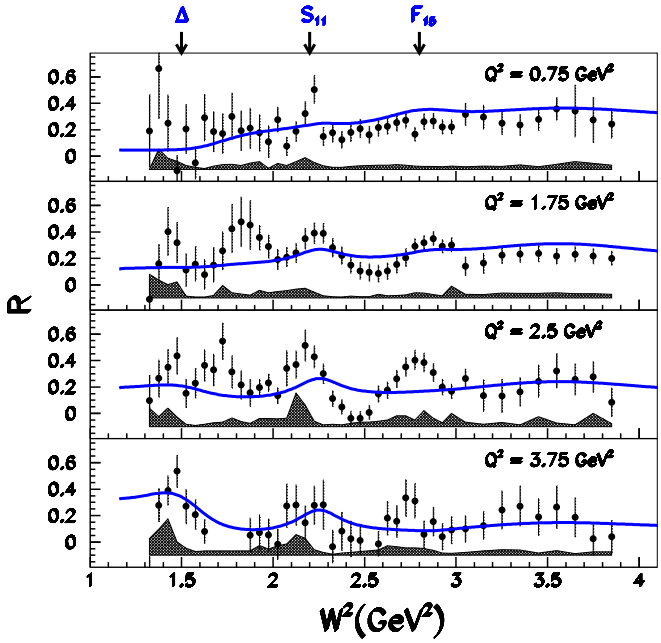

FIG. 2. Measurements of $R = \sigma_L/\sigma_T$, as a function of W^2, for the Q^2 values indicated. The error bars shown represent both the statistical and uncorrelated systematic uncertainties, with the former negligible in comparison to the latter. The shaded band below the offset zero represents the total scale uncertainty and the blue curve is the fit of Ref. [31]. The locations of the three prominent resonances observed in the unseparated cross-section measurements are labeled at the top.

3.0 GeV^2 and ± 0.10 GeV^2 for $W^2 \geqslant 3.0$ GeV^2 were brought to a central value using a fit. (Larger ranges were employed at the higher W^2 values where the cross section becomes less W^2-dependent.) Different fits were utilized to assess any model-dependent uncertainty in this step which was typically less than 3% [25]. This uncertainty concern dictated that separations were not performed if the required centering correction was larger than 60%.

IV. RESULTS AND INTERPRETATION

Values obtained for R are plotted versus W^2 in Fig. 2 for the Q^2 values indicated, along with the fit from Ref. [31]. It is clear from the mass enhancements in the data that R exhibits resonant structure, and that this variation with W^2 can be quite large. This is the first direct observation of such structure, contradicting a common assumption that the resonance contribution to R, or the longitudinal strength in the resonance region, is small or negligible (for example, Refs. [33–39]). There are very few calculations for R in the resonance region, and not all of those include explicit resonance contributions or have both the longitudinal and transverse response needed to extract R. Therefore, we will compare our data to existing calculations for the separated structure functions F_1 and F_L rather than for R.

The almost 20 well-established nucleon resonances with masses below 2 GeV give rise to only three distinct enhancements in the unseparated inclusive electron scattering cross section and, of the three, only the first (the lowest mass $P_{33}(1232)$, Δ) state is not a superposition of overlapping resonant states. The second enhancement region is often referred to as the S_{11}, as the unseparated cross section here is dominated above $Q^2 \approx 1$ GeV^2 by the ground state $S_{11}(1535)$ resonance, even though there exists the $D_{13}(1520)$ overlapping resonance. A similar situation is true for the third enhancement region, which is dominated by the $F_{15}(1680)$, with even more overlapping resonance states. In R, however, the situation appears to be different. There is an additional prominent peak at $W^2 \approx 1.8$ GeV^2, somewhat below the S_{11} dominated mass region.

The lowest mass Δ resonance region exhibits nonnegligible longitudinal strength over the full Q^2 range of this experiment, albeit with limited statistical precision at the lowest Q^2 value shown. The spin-flip required for this positive parity isospin $I = 3/2$ excitation suggests that it be dominantly transverse, yet some models predict a possible nonnegligible longitudinal component [40–44]. Recent analyses of predominantly exclusive scattering data from JLab [45–47] differ somewhat but generally tend to indicate a small longitudinal Δ resonant component. It has been noted that Rosenbluth separated data such as that presented here will be critically useful input to such analyses [48]. It is also possible that the R values observed here may indicate a substantial nonresonant background contribution in this regime.

The possible peak observed in R at $W^2 \approx 1.8$ GeV^2 in Fig. 2 below the S_{11} is notable, albeit with large uncertainty, in the F_L longitudinal channel. This mass is close to that of the elusive Roper resonance, $P_{11}(1440)$, the electroproduction of which is a topic of significant interest [49–55]. The excitation of the Roper resonance has been found to be dominantly longitudinal [46]. The observed mass is also near the P_{13}, or $\Sigma(1385)$, resonance. This resonance should have a small cross section in electroproduction, but could show up preferentially in the longitudinal channel which is dominant in kaon production. Regardless of its origin, this is a surprising observation of significant resonant longitudinal strength, and bears further experimental and theoretical investigation.

In all, the data clearly exhibit differing longitudinal and transverse resonance behavior, as shown in Fig. 3, where the purely transverse $2xF_1$ and purely longitudinal F_L structure functions are plotted separately. Here, the structure functions are plotted as a function of x rather than W, for the purpose of further discussions below. The mass peak regions move up in x with increasing Q^2. It may be observed that there are mass peaks in *both* the longitudinal and transverse channels, and that the peak positions differ somewhat. Not only do the data unequivocally demonstrate significant longitudinal resonance structure, but the W-dependence (or x dependence) of F_L is larger than that of $2xF_1$ above $Q^2 \approx 1$ GeV^2, as evidenced by the relatively greater prominence of the mass peaks in the bottom panel of Fig. 3.

A precise extraction of information on individual resonances, such as transition form factors, from these inclusive data must involve a detailed fitting study beyond the scope of this report. At lower values of $Q^2 < 1$ GeV^2, unitary isobar fits like MAID [56] give quite definite and accurate predictions based on single pion, two pion, eta, and kaon decay

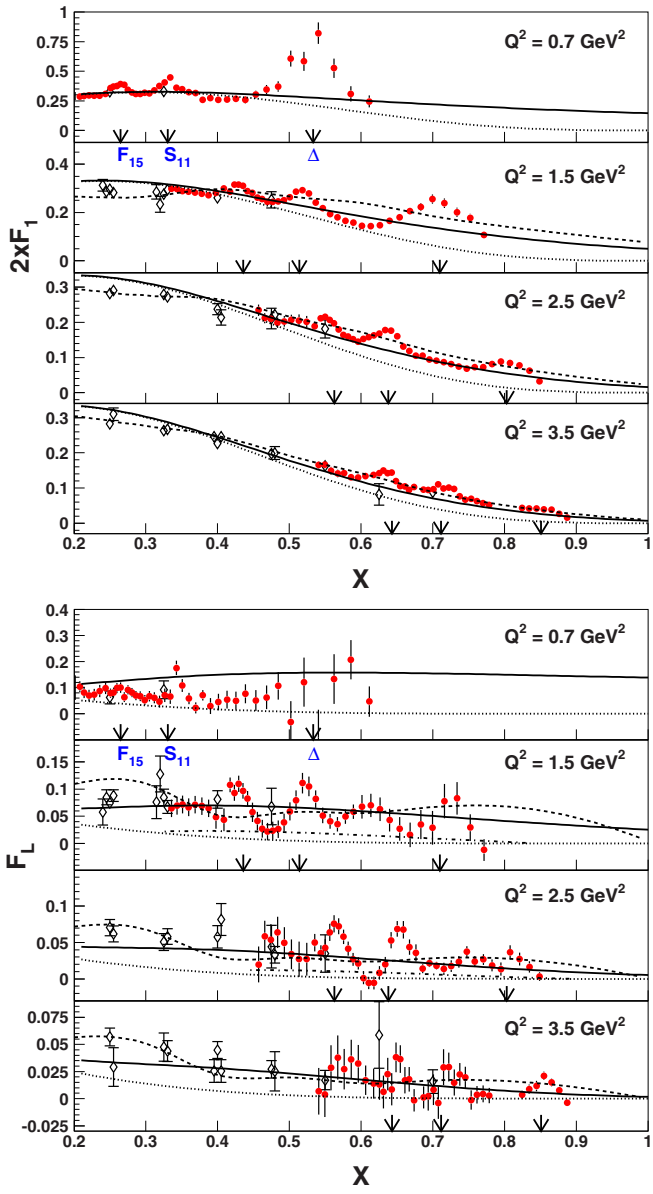

FIG. 3. The longitudinal structure function F_L (top), and transverse nucleon structure function $2xF_1$ (bottom), measured in the resonance region (triangles) as a function of x, compared with existing DIS measurements from SLAC (diamonds). The curves are from MAID (bottom middle, dot-dashed), Alekhin (dashed), and MRST with (solid) and without (dotted) target mass effects included. The three prominent resonance mass regions observed in the inclusive cross section are indicated by arrows, and labeled in the top plots. The error bars shown represent both the statistical and systematic uncertainties, with the latter being dominant.

channels for resonances below $W^2 < 4$ GeV^2. At the higher Q^2 values of the data presented here, however, multipion effects, tails of higher mass resonances, and nonresonant components are very significant and therefore such fits tend to underestimate this data, as can be seen from the MAID curve in Fig. 3 (bottom).

Also presented with the resonance region data in Fig. 3 are the predominantly DIS ($W^2 > 4$ GeV^2) data from Rosenbluth separations performed at SLAC [5,6]. Where overlapping, the two data sets are in agreement, providing additional confidence in the achievement of the demanding precision required for these experiments. In all cases, there is a smooth transition between the resonance and DIS data in both x and Q^2.

The curves shown are parton distribution based parametrizations of structure functions at next-to-next-to leading order, from Alekhin [57], including target mass effects according to Ref. [58], and from MRST [59], both with and without target mass effects according to Refs. [60,61]. The MRST parametrization includes data from deep inelastic scattering as well as other experiment types, while Alekhin's calculation uses only DIS. The latter calculation is valid only down to $Q^2 = 1$ GeV^2.

It is clear that some prescription for target mass effects is required to describe the data. However, for $Q^2 > 1$ GeV^2, it appears that minimal if any additional nonperturbative descriptions (such as higher twist effects) seem necessary to describe the *average* behavior of the resonance region. The resonances oscillate around the scaling curves. Furthermore, this is true for the range of different Q^2 values, indicating that the scaling curve describes as well the average Q^2 dependence of the resonance regime. These observations are consistent with quark-hadron duality [22], and may be counted as the first observation of duality in the separated transverse and longitudinal structure functions.

V. CONCLUSIONS

In summary, we have reported results from a first detailed study of longitudinal and transverse strength in the nucleon resonance region. The new data have yielded an array of interesting observations. Contrary to most transition form factor fit assumptions, the resonant longitudinal component is found to be substantial. Furthermore, the resonance mass dependence of the longitudinal structure function is more pronounced than the transverse. Significant strength is observed between the S_{11} and Δ resonance mass regions in the longitudinal channel. Separated measurements of the inelastic structure functions F_1 and F_L are presented. The data show quark-hadron duality for the first time in the F_1 and F_L structure functions independently.

These data are now available [62] for additional studies.

ACKNOWLEDGMENTS

We gratefully acknowledge support from the U.S. Department of Energy, Office of Science, Office of Nuclear Physics (including Grants No. DE-AC02-05CH11231 and No. DE-AC02-06CH11357) and the National Science Foundation. We thank the Jefferson Lab Hall C scientific and engineering staff for their outstanding support. The Southeastern Universities Research Association operates the Thomas Jefferson National Accelerator Facility under the US Department of Energy Contract No. DE-AC05-84ER40150.

[1] A. Bodek, M. Breidenbach, D. L. Dubin, J. E. Elias, J. I. Friedman, H. W. Kendall, J. S. Poucher, E. M. Riordan, M. R. Sogard, D. H. Coward *et al.*, Phys. Rev. D **20**, 1471 (1979).

[2] C. Callan and D. Gross, Phys. Rev. Lett. **22**, 156 (1969).

[3] V. Tvaskis, M. E. Christy, J. Arrington, R. Asaturyan, O. K. Baker *et al.*, Phys. Rev. Lett. **98**, 142301 (2007).

[4] L. W. Whitlow, S. Rock, A. Bodek, E. M. Riordan, and S. Dasu, Phys. Lett. B **250**, 193 (1990).

[5] S. Dasu, P. deBarbaro, A. Bodek, H. Harada, H. Krasny, K. Lang, E. M. Riordan, L. Andivahis, R. Arnold, D. Benton *et al.*, Phys. Rev. D **49**, 5641 (1994).

[6] L. H. Tao *et al.*, Z. Phys. C **70**, 387 (1996).

[7] C. Adloff *et al.* (H1 Collaboration), Phys. Lett. B **393**, 452 (1997).

[8] R. P. Feynman, *Photon-Hadron Interactions* (W. A. Benjamin, Reading, MA, 1976).

[9] I. Niculescu, C. S. Armstrong, J. Arrington, K. A. Assamagan, O. K. Baker *et al.*, Inclusive resonance electroproduction data from hydrogen and deuterium and studies of bloom-gilman duality, Ph.D. thesis, Hamption University, 1999.

[10] V. Tvaskis, A. Tvaskis, I. Niculescu, D. Abbott, G. S. Adams *et al.*, Phys. Rev. C **97**, 045204 (2018).

[11] K. Ackerstaff *et al.* (HERMES Collaboration), Phys. Lett. B **475**, 386 (2000); Erratum: **567**, 339 (2003).

[12] A. Sheren, Measurement of the Nuclear Dependence of F_2 and $R = \sigma_L/\sigma_T$ in the Nucleon Resonance Region, Ph.D. thesis, Kent State University, 2019.

[13] A. Bodek and C. Keppel, Measurements of F_2 and R on Nuclear Targets in the Resonance Region, Jefferson Lab Experiment E04-001 (2004).

[14] G. Altarelli and G. Martinelli, Phys. Lett. B **76**, 89 (1978).

[15] R. K. Ellis *et al.*, Nucl. Phys. B **207**, 1 (1982).

[16] R. K. Ellis *et al.*, Nucl. Phys. B **212**, 29 (1982).

[17] I. Niculescu, C. S. Armstrong, J. Arrington, K. A. Assamagan, O. K. Baker, D. H. Beck, C. W. Bochna, R. D. Carlini, J. Cha, C. Cothran *et al.*, Phys. Rev. Lett. **85**, 1186 (2000).

[18] I. Niculescu, C. S. Armstrong, J. Arrington, K. A. Assamagan, O. K. Baker, D. H. Beck, C. W. Bochna, R. D. Carlini, J. Cha, C. Cothran *et al.*, Phys. Rev. Lett. **85**, 1182 (2000).

[19] J. Arrington, R. Ent, C. E. Keppel, J. Mammei, and I. Niculescu, Phys. Rev. C **73**, 035205 (2006).

[20] S. P. Malace, G. S. Adams, A. Ahmidouch, T. Angelescu, J. Arrington *et al.*, Phys. Rev. C **80**, 035207 (2009).

[21] N. Bianchi, A. Fantoni, and S. Liuti, Phys. Rev. D **69**, 014505 (2004).

[22] W. Melnitchouk, R. Ent, and C. Keppel, Phys. Rep. **406**, 127 (2005).

[23] M. E. Christy and C. Keppel, Measurement of $R = \sigma_L/\sigma_T$ in the Nucleon Resonance Region, Jefferson Lab Experiment E94-110 (1994).

[24] M. E. Christy *et al.* (E94110 Collaboration), Phys. Rev. C **70**, 015206 (2004).

[25] Y. Liang, Measurement of $R = \sigma_L/\sigma_T$ in the Nucleon Resonance Region, Ph.D. thesis, The American University, 2003.

[26] C. E. Keppel, Inclusive Nucleon Resonance Electroproduction at Large Momentum Transfer, Ph.D. thesis, The American University, 1994.

[27] P. E. Bosted, Phys. Rev. C **51**, 409 (1995).

[28] J. Arrington, Phys. Rev. C **69**, 022201(R) (2004).

[29] J. Arrington, P. G. Blunden, and W. Melnitchouk, Prog. Part. Nucl. Phys. **66**, 782 (2011).

[30] V. Tvaskis, J. Arrington, M. E. Christy, R. Ent, C. E. Keppel, Y. Liang, and G. Vittorini, Phys. Rev. C **73**, 025206 (2006).

[31] M. E. Christy and P. E. Bosted, Phys. Rev. C **81**, 055213 (2010).

[32] M. N. Rosenbluth, Phys. Rev. **79**, 615 (1950).

[33] P. Stoler, Phys. Rep. **226**, 103 (1993).

[34] L. M. Stuart, P. E. Bosted, L. Andivahis, A. Lung, J. Alster, R. G. Arnold, C. C. Chang, F. S. Dietrich, W. R. Dodge, R. Gearhart *et al.*, Phys. Rev. D **58**, 032003 (1998).

[35] M. M. Dalton *et al.*, Phys. Rev. C **80**, 015205 (2009).

[36] K. Joo *et al.*, Phys. Rev. Lett. **88**, 122001 (2002).

[37] N. F. Sparveris, R. Alarcon, A. M. Bernstein, W. Bertozzi, T. Botto, P. Bourgeois, J. Calarco, F. Casagrande, M. O. Distler, K. Dow *et al.*, Phys. Rev. Lett. **94**, 022003 (2005).

[38] V. V. Frolov, G. S. Adams, A. Ahmidouch, C. S. Armstrong, K. Assamagan, S. Avery, O. K. Baker, P. Bosted, V. Burkert, R. Carlini *et al.*, Phys. Rev. Lett. **82**, 45 (1999).

[39] F. Kalleicher, U. Dittmayer, R. W. Gothe, H. Putsch, T. Reichelt, B. Schoch, and M. Wilhelm, Z. Phys. A **359**, 201 (1997).

[40] P. Kroll, M. Schurmann, and W. Schweiger, Z. Phys. A **342**, 429 (1992).

[41] N. Isgur, G. Karl, and R. Koniuk, Phys. Rev. D **25**, 2394 (1982).

[42] U. Meyer, E. Hernandez, and A. J. Buchmann, Phys. Rev. C **64**, 035203 (2001).

[43] S. S. Kamalov and S. N. Yang, Phys. Rev. Lett. **83**, 4494 (1999).

[44] M. Fiolhais, G. Golli, and S. Sirca, Phys. Lett. B **373**, 229 (1996).

[45] I. G. Aznauryan *et al.* (CLAS Collaboration), Phys. Rev. C **80**, 055203 (2009), and references therein.

[46] J. J. Kelly, O. Gayou, R. E. Roche, Z. Chai, M. K. Jones *et al.*, Phys. Rev. C **75**, 025201 (2007), and references therein.

[47] I. G. Aznauryan *et al.*, Int. J. Mod. Phys. E, **22**, 1330015 (2013).

[48] J. J. Kelly, Phys. Rev. C **72**, 048201 (2005); **72**, 059901(E) (2005).

[49] K. Joo *et al.* (CLAS Collaboration), Phys. Rev. C **70**, 042201 (2004).

[50] T. S. Lee and L. C. Smith, J. Phys. G: Nucl. Part. Phys. **34**, S83 (2007).

[51] L. Alvarez-Ruso, M. B. Barbaro, T. W. Donnelly, and A. Molinari, Nucl. Phys. A **724**, 157 (2003).

[52] Z. P. Li, V. Burkert, and Z. J. Li, Phys. Rev. D **46**, 70 (1992).

[53] S. R. Beane and U. van Kolck, J. Phys. G: Nucl. Part. Phys. **31**, 921 (2005).

[54] R. D. Matheus, F. S. Navarra, M. Nielsen, R. Rodrigues da Silva, and S. H. Lee, Phys. Lett. B **578**, 323 (2004).

[55] R. L. Jaffe and F. Wilczek, Phys. Rev. Lett. **91**, 232003 (2003).

[56] D. Drechsel, S. S. Kamalov, and L. Tiator, Nucl. Phys. A **645**, 145 (1999); Eur. Phys. J. A **34**, 69 (2007).

[57] S. I. Alekhin, Phys. Rev. D **68**, 014002 (2003).

[58] H. Georgi and H. D. Politzer, Phys. Rev. Lett. **36**, 1281 (1976); **37**, 68(E) (1976); Phys. Rev. D **14**, 1829 (1976).

[59] A. D. Martin, R. G. Roberts, W. J. Stirling, and R. S. Thorne, Eur. Phys. J. C **18**, 117 (2000).

[60] R. Barbieri, J. R. Ellis, M. K. Gaillard, and G. G. Ross, Nucl. Phys. B **117**, 50 (1976).

[61] I. Schienbein *et al.*, J. Phys. G: Nucl. Part. Phys. **35**, 053101 (2008).

[62] Data are available at http://hallcweb.jlab.org/resdata.